THE DIRECT SIMULATION OF HIGH-SPEED MIXING-LAYERS WITHOUT AND WITH CHEMICAL HEAT RELEASE

B. Sekar *, H.S. Mukunda †, M.H. Carpenter ‡

ABSTRACT

This computational study is a direct numerical simulation of high speed reacting and non-reacting flows for H_2-air systems. The calculations are made for a convective Mach number of 0.38 with hyperbolic tangent initial profile and finite rate chemical reactions. A higher-order numerical method is used in time accurate mode to time advance the solution to a statistical steady state. About 600 time slices of all the variables are then stored for statistical analysis.

It is shown that most of the problems of high-speed combustion with air are characterized by relatively weak heat release. The present study shows that (i) the convective speed is reduced by heat release by about 10 % at this convective Mach number $M_c = 0.38$, (ii) the variation of the mean and rms fluctuation of temperature can be explained on the basis of temperature fluctuation between the flame temperature and the ambient, (iii) the growth rate with heat release is reduced by 7 %, (iv) and the entrainment is reduced by 25 % with heat release. These differences are small in comparison with incompressible flow dynamics, and are argued to be due to the reduced importance of heat release in comparison with the large enthalpy gradients resulting from the large-scale vortex dynamics. It is finally suggested that the problems of reduced mixing in high-speed flows are not severely complicated by heat release.

NOMENCLATURE

M	:	Mach number	M_c	:	Convective Mach number
p	:	Pressure	Re	:	Reynolds number
T	:	Temperature	T'	:	Root mean square fluctuation of T
t	:	Time	$tanh$	:	Tanhyperbolic
u	:	Streamwise velocity	u'	:	Root mean square fluctuation of u
u_∞	:	Primary stream velocity	$u_{-\infty}$	:	Secondary stream velocity
u_c	:	Convective velocity	v	:	Transverse velocity
x	:	Streamwise coordinate	x_m	:	Maximum extent of x field
y	:	Transverse coordinate	y_m	:	Maximum extent of y field
δ	:	Mixing-layer thickness	ρ	:	Density
Ω	:	Vorticity	μ	:	Laminar viscosity

INTRODUCTION

Non-reacting and reacting incompressible mixing-layers have been extensively explored both experimentally (ref. 1-3) and computationally (ref. 4,5). Laboratory experiments have shown that the growth of the mixing-layer is dominated by large-scale quasi-two-dimensional vortices and their pairing in the early stages. A non-reacting spatial simulation of the incompressible mixing-layer carried out by McInville et al. (ref. 4), found that the growth of the layer with axial distance shows an occasional decrease to an extent of 10 %. This has been argued to be due to the phase

*Research Scientist, Vigyan Research Associates, Hampton, VA. Research funded under contract NAS1-18585 from NASA Langley.
†Professor, Indian Institute of Science, Bangalor, India. Work performed while in residence at NASA Langley as NRC fellow.
‡Aerospace Engineer, Theoretical Flow Physics Branch, Fluid Mechanics Division, NASA Langley Research Center, Hampton, VA.

relationships between the initial disturbance and the evolution of the roll up of the vortical structure downstream. Under suitable phase conditions the energy of the fluctuating part is drawn away into the mean flow thus decreasing the growth of the layer.

For reacting mixing-layers, the results of Hermanson and Dimotakis (ref. 2), also quoted in McMurtry et al. (ref. 5) for their experiments classified as "weak heat release" cases with the peak to initial temperature ratio being 2.3 and 4 respectively, show that heat release results in a slightly reduced growth of the shear-layer (of the order of 10 - 15 %). This result has been related to the reduction in turbulent shear stresses in the layer. Though the spacing of the cores of vortical structures has been shown not to be affected by heat release (p.11, ref.5), this result seems to have been accepted with reservation. McMurtry et al. (ref. 5) have conducted accurate temporal simulations of low Mach number flows without and with heat release. These have confirmed the experimental findings regarding the slower growth of the layer with heat release. Analysis seems to indicate the important role of thermal expansion and baroclinic torque in reducing the peak vorticity generation within the layer, thereby reducing the molecular diffusion.

All the results noted above are for near incompressible flows. Supersonic mixing-layers have been explored experimentally by Papamoschou and Roshko (ref. 6) who showed that the growth rate decreases with an increase in the convective Mach number (M_c); M_c is the ratio of the difference in the velocities of the two streams to the sum of the acoustic speeds in the upper and lower streams. The reduction in the growth rate is shown to be related to the reduced amplification of the disturbances in supersonic flows (ref. 7). Lele (ref. 8) made direct simulation calculations of supersonic flows using higher-order finite difference methods and validated the concept of M_c. Mukunda et al. (ref. 9) made similar calculations for non-reacting flows first establishing the results of Papamoschou and Roshko (ref. 6) and then exploring the influence of initial profile (hyperbolic tangent and wake like profiles), the disturbance level and nature on the development of the mixing-layer. All these studies were restricted to non-reacting flows. The present work aims at elucidating the effects of chemical heat release in high-speed flows.

MOTIVATION

The origin of the present problem lies in the recent interest in the development of the propulsion system for the national aerospace plane. The typical flight Mach numbers can be as high as 21 and in the combustor up to 7. The combustor inlet temperatures are 1500-2500 K and pressures are 0.05 to 0.15 MPa. At these conditions the reaction rates are very high and the steady combustion will be limited by mixing. The findings of reduced mixing in shear flows (i) due to high M_c (ref. 6) and (ii) due to heat release in incompressible flows (ref. 2,3) have caused concern in the development of combustors for high-speed flows and need for a basic examination of reacting high-speed flows. The present contribution considers a typical case (ref. 10) of a high-speed mixing-layer.

The fuel-oxidizer combination used is N_2 diluted H_2-air. In the present study, the case with 10 % (mass) H_2 in N_2 is treated in continuation with the earlier studies by Drummond and Mukunda (ref. 10). The relevance of a study with a low fraction of hydrogen can be justified by analyzing the importance of the extent of heat release. In incompressible flows, one would obtain substantial variation in adiabatic flame temperature, T_{ad} (a good estimate of possible peak temperatures in the flame) by adjusting the hydrogen mass fraction Y_{H_2} in the N_2 stream. The ratio s ($= T_{ad} / T_{in}$, where T_{in} is the initial temperature) for $T_{in} = 300$ K would be about 8 for pure H_2 and about 7 for $Y_{H_2} = 0.1$. For high-speed applications, the magnitude of this trend is greatly reduced. Computation of T_{ad} shows that with $T_{in} =$ 2000 K, s = 1.6 for pure H_2 and 1.57 for $Y_{H_2} = 0.1$. Two important facts from these values are that (i) the T_{ad} is virtually the same for pure and diluted H_2, and (ii) the temperature ratio is not large. In fact, it is lower than the values used for the case of weak heat release in the experiments (see ref. 5). The reason "s" does not differ greatly between $Y_{H_2} = 1.0$ and 0.1 is that most of the energy input goes into the dissociation of the species including N_2 and the formation of energy absorbing NO. Though the present work treats N_2 as an inert, the use of a reversible reaction limits the peak temperature to s = 1.575, a value close to that from full chemistry.

THE COMPUTATIONAL ASPECTS

The geometry considered here is shown in figure (1). The computational box ABCD has an x and y dimension of x_m and y_m, respectively. The inflow boundary profile (A-D) is divided into two domains at the point $y = y_m/2$. The

top section is the fuel region and the bottom, air. The inflow velocity is the hyperbolic tangent profile conventionally used in mixing-layer studies given by $u_m = \frac{1}{2}[(u_\infty + u_{-\infty}) + (u_\infty - u_{-\infty})tanh\ ky]$ with the constant k taken here as 1800 m^{-1}. This results in an effective boundary-layer thickness of two millimeters, based on a 99 % freestream criterion.

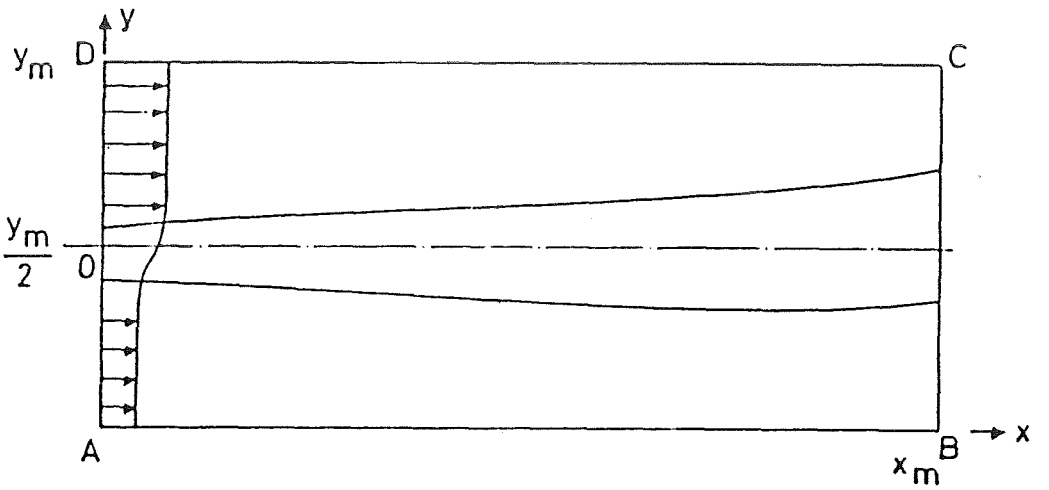

Figure 1: Schematic of mixing-layer.

Table 1 shows the parameters relevant to the cases considered. The velocity of the air stream is lower than that of the fuel in the case $M_c = 0.38$. The momentum ratios indicate that the momenta are balanced for $M_c = 0.38$. This causes the shear-layer to remain roughly in alignment with the central axis. The momentum defect thickness(θ) is 1.54 mm. This implies that for the x grid length of 100 mm, the axial span is about 64 θ. The Re_δ based on the average properties is 3500. If the reference speed is the difference in speeds between the streams, then Re is 250. These values are considered low enough to obtain realistic results using direct simulations with the current day computational resources for non-reacting flows. It is for this range of values that Lele (ref. 8) has made direct simulation computations. Chemical reactions will certainly introduce scales which are smaller than those present in non-reacting flows. It is hoped that the essential features of the reaction will still be resolved.

Disturbances are provided on the axial and lateral velocities (u_d and v_d)at x = 0 to excite the layer. The disturbance is composed of a linear combination of several harmonic components of frequency determined from a spectral analysis of the flow field (at a downstream region) computed without any initial disturbances. The initial rms "u" fluctuation is about 3.68 %. The boundary conditions on (A-D) would be u= $u_m + u_d$, v=v_d, p=0.101325 MPa, T= 2000 K and

$$\begin{aligned} Y_{H_2} = 0.1,\ Y_{O_2} = \ Y_{H_2O} = 0.0,\ Y_{N_2} = 0.9, (y_m > y > y_m/2) \\ Y_{O_2} = 0.232, Y_{H_2} = \ Y_{H_2O} = 0.0,\ Y_{N_2} = 0.768, (y_m/2 > y > 0) \end{aligned} \quad (1)$$

At x = x_m, third order extrapolation of the primitive variables is used. At y = 0 and y_m, characteristic boundary conditions are used to obtain the extrapolated primative variables.

After a detailed study (ref. 9), the region of calculation was chosen as 100 mm × 50 mm. In order to capture most scales of importance, the grid distribution is chosen by considerations outlined in reference 9 and partly based on the discussion of Reynolds (ref. 11). The number of gridpoints used in the y direction is 125 or 151 for a region of 50 mm and are concentrated near the center of the layer. The x direction (100 mm) is embedded with 201 or 251 equi-spaced gridpoints resulting in a axial spacing of 0.5 - 0.4 mm. Calculations have been made to ensure grid independence of several details of the flow (ref. 9).

The code used in the present calculations is the SPARK2D combustion code developed at NASA Langley over

Table 1: INFLOW PARAMETERS

composition	quantity	case 1
Fuel $0.1H_2 + 0.9N_2$	ρ, kg/m^3	0.075
	u, m/s	2670.0
	M	2.0
	γ	1.3133
	sound speed, m/s	1336.0
	δ, mm	1.0
	μ, kg/m.s	5.5 $\times 10^{-5}$
Oxidant $0.232O_2 + 0.768N_2$	ρ, kg/m^3	0.175
	u, m/s	1814.0 .0
	M	2.1
	γ	1.296
	sound speed, m/s	864.3
	δ, mm	1.0
	μ, kg/m.s	6.2 $\times 10^{-5}$
	u_c, m/s	2150.0
	M_c	0.385

T = 2000 K, p = 0.101325 MPa, θ = 1.54 mm

the past four years by Drummond and Carpenter(see refs 10, 12 and 13). In the latest version (ref. 12), it uses either a third-order upwind biased or a dissipative compact fourth-order central difference algorithm (DCPS) for the streamwise direction, and the DCPS (ref. 13) for the cross-stream direction. The temporal accuracy is second order. This choice represents a compromise between the accuracy of higher-order numerical algorithms and the robustness and efficiency of lower-order methods.

In addition to full finite rate chemical kinetics, two simplified reaction models were used in this study. The purpose was to evaluate the validity of the simplified reaction models at these flow conditions with respect to the more general full chemistry model. The first is $2H_2 + O_2 \rightleftharpoons 2H_2O$, and the reaction rate is given by

$$\dot{\omega}''' = A_f p^2 Y_{H_2}^2 Y_{O_2} e^{-E_f/RT} - A_b p Y_{H_2O}^2 e^{-E_b/RT} \tag{2}$$

Here the backward rate constant in the above equation is chosen to be consistent with the equilibrium constant. The parameters of the forward rate constant are taken as $A_f = 1.1 \times 10^{19}$, and an activation energy, $E_f = 16$ kcal / mole. These values were obtained by requiring that the flame speed of the single step kinetics match with those from full chemistry. The second reaction model chosen is a seven species, seven reaction path model involving H_2, O_2, H_2O, OH, H, O, and passive N_2. This model is the reaction system given by Drummond (ref. 10) abridged to the major species at these temperatures. The species and their reactions usually included to predict ignition onset (HO_2 and H_2O_2) are neglected for computational efficiency. A binary diffusion model was used for all calculations with a single representative Schmidt number of 0.22, the value generally used for the diffusion of H_2. This has been taken so as to obtain a reference case for comparison with subsequent calculations on the effect of multi-component diffusion of various species.

In order to ensure that the flow attains a statistical steady state before sampling is performed, the computations were performed for each case for a duration of about three sweeps of the flow. Each sweep takes a time given by x_m/u_c. This is about 50 μs for the $M_c = 0.38$ case. The time step is typically 0.005 μs and, therefore, takes 20000 - 30000 time steps before statistical steady state is achieved. After this, a total of about 600 time samples of all the flow field variables at specific x and y stations are stored at equal time intervals. These are subsequently analyzed by a separate statistical package. The results from this package include the mean and correlation quantities. The shear-layer thickness was obtained for "u", ρ, Y_{H_2}, Ω, and Y_{H_2O}. Of these, Y_{H_2O} and Ω tend to zero at y $\rightarrow \pm\infty$;

the others tend to nonzero finite values. In view of these features, the thicknesses are defined by

$$\delta_\psi = \frac{(\psi_\infty - \psi_{-\infty})}{(\partial \psi_{mean}/\partial y)_{max}} \tag{3}$$

where ψ stands for any of the first three quantities. For Y_{H_2O} and Ω, $\delta_\psi = \int_{-\infty}^{\infty} \psi dy \,/\, \psi_{max}$.

The speed of vortical structures expected to be at the convective speed (u_c) is obtained by making instantaneous p vs x plots at some value of y near the center of the mixing-layer. These plots are made at a few times sufficiently spaced apart. The rate of movement of the point of peak pressure along x gives the convective speed. The convective speed is also calculated by using the formula (ref. 6),

$$u_c = \frac{\sqrt{\rho_{-\infty}}u_{-\infty} + \sqrt{\rho_\infty}u_\infty}{(\sqrt{\rho_\infty} + \sqrt{\rho_{-\infty}})} \tag{4}$$

CODE VALIDATION

The first step in validating the code was to determine if the numerical methods used in the SPARK2D code are capable of resolving the linear growth of the two-dimensional mixing-layer. It is essential that for grids comparable to those used in this study, all the aspects of the linear regime of the mixing-layer be well resolved, before addressing the far more difficult non-linear problem of vortex role-up and chemical reaction. Linear stability theory predicts that the temporally developing compressible 2-D mixing-layer (air into air, in this case), is unstable to a velocity profile which is initially specified as a hyperbolic tangent axial velocity distribution. In the initial stages of the instability (the linear regime), the growth of the unstable modes is exponential. For these calculations, accurate eigenmodes were provided from a spectral linear stability code developed by Macaraeg (ref. 14). From these eigenmodes, nondimensional growth rates and characteristic frequencies were calculated. This non-dimensional growth rate provided a reliable measure of the accuracy of the finite-difference algorithm being tested.

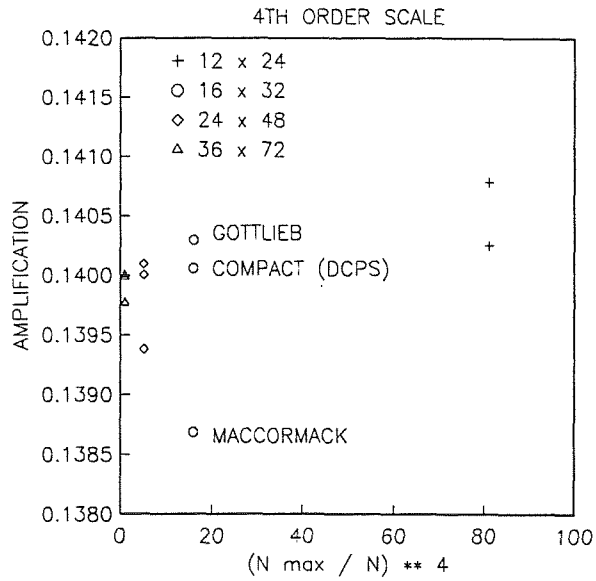

Figure 2: Grid convergence study for the temporal growth of the two-dimensional mixing-layer.

The temporal growth of the two-dimensional mixing-layer is simulated by assuming the flow to be periodic in the stream-wise direction. The period corresponds to a wavelength of x = 0.6283mm (the mode which grows most rapidly, as determined from the linear analysis). The initial velocity distribution is specified as $U(x, y, 0) = u_\infty \tanh(\frac{y}{\delta})$, v(x,y,0) = 0.0, T(x,y,0) = $293^o k$, p(x,y,0) = 0.101325 MPa. Source terms were added to the Navier-Stokes equations so that the momentum and energy equations would preserve free-stream. The resulting Reynolds number of the flow

is 187, based on the layer thickness, where U_∞ = 100 m/s. The Mach number is 0.30. The width of the half-layer D is specified to be $2.5x10^{-2}$mm and the half-width of the domain is 100 times the layer thickness. The grid in the stream-wise direction is uniform, while the grid in the cross-stream direction is highly stretched. The transformation of the grid ensures that about one half of all the y grid-points are located within the initial mixing-layer width.

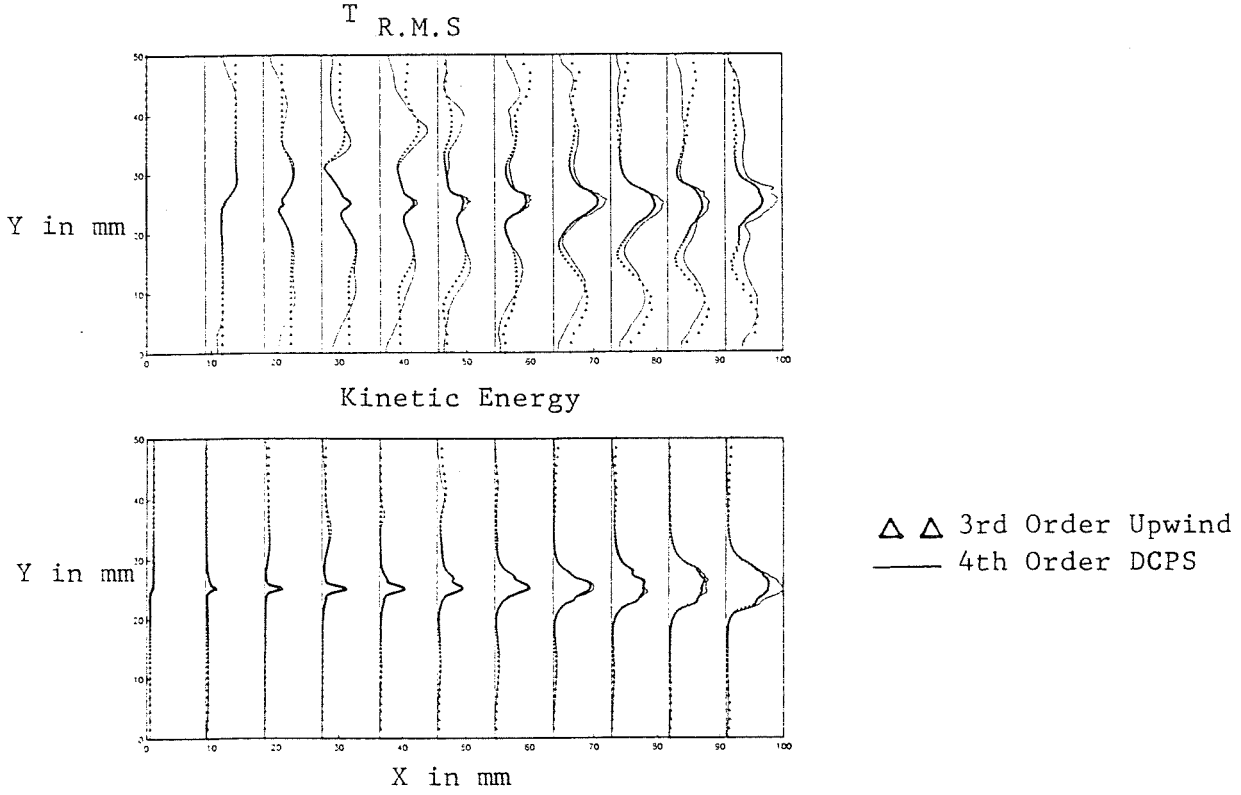

Figure 3: Comparison of a) r.m.s temperature profiles and b) Kinetic energy fluctuating statistics calculated with third and fourth-order numerical methods.

For these studies the unstable modes in the layer were allowed to grow from the numerical instabilities produced by machine roundoff errors. Exponential growth of these modes was seen in all cases after an initial transient period. The "linear" regime was characterized by the growth period during which the product of perturbation quantities was still negligible. For these tests this period was arbitrarily chosen between the physical times of $2.5x10^{-5}$ and $2.75x10^{-5}$ seconds, and corresponded to disturbance amplitudes three to five orders larger than machine roundoff errors. A grid convergence history of the numerical method was used to determine its formal accuracy, and to ascertain the grids necessary to resolve this fundamental phenomena.

The most unstable mode in this problem grows at an exponential growth rate with an exponent determined from linear stability theory to be 0.14000 in non-dimensional units. This rate was used as the "exact" growth rate for these conditions. A series of four grids was then defined, each having a grid density which was a constant multiple of the previous grid. Three algorithms: 1) MacCormack at a CFL of 1.0, 2) Gottlieb-Turkel (ref. 15) at a CFL of 0.5, and 3) DCPS at a CFL of 0.5, were then run on identical grids and the non-dimensional amplification rate was determined from an integration of the energy spectrum. (The integral of the fundamental mode over the entire domain was monitored in time. The change with respect to time yields the amplification rate).

In figure (2) the amplification rates of the three methods are plotted against $(\frac{N_{max}}{N})^4$ (where N_{max} and N are the maximum number of gridpoints used in the study and the number used on a particular coarser grid, respectively) to show quartic accuracy. Here, the fourth-order spatial accuracy of the spatial derivatives from each method is indicated by the linear convergence of the solution to the predetermined amplification rate. The Gottlieb-Turkel scheme and the DCPS both converge with fourth-order accuracy. (This indicates that the coefficients multiplying the temporal terms of $O(\Delta t^2)$ and $O(\Delta t \Delta x^2)$ in the methods, are small compared with the spatial truncation terms). A direct comparison

of the accuracy of the two fourth-order methods can be drawn, since the only variable in this study was the method used. The DCPS appears to be about twice as accurate as the the Gottlieb-Turkel scheme for this problem. From these results it is apparent that, even for coarse grids (10 grid-points per wavelength), the fundamental features of the linear growth of the mixing-layer are resolved. There should be no question that the grids used in these studies are sufficient to resolve the linear regime of the two-dimensional mixing-layer.

Showing appropriate grid resolution for the non-linear case is far more difficult. In addition to grid convergence studies for a representative flow, a direct comparison of two numerical methods was used to measure the grid independence of the solutions. The similarity of solutions obtained on the same grid from numerical methods having different truncation errors, provides a measure of the solution convergence on that grid (for the methods being used). In this vein, a third-order upwind-biased method was compared with the fourth-order DCPS central difference scheme on a 201 x 151 grid. Both were run to the same physical time and statistics of the flow were gathered for each case. The mean profiles calculated with each method do not show any appreciable differences. However, small changes in the fluctuating quantities are present. Figure (3a) shows the r.m.s temperature profiles for the flow as calculated with each method. Figure (3b) shows a comparison of the kinetic energy statistics gathered from each simulation. While the qualitative features of the statistics are reproduced with each method, they are not quantitatively the same. (The dissipative nature of the third-order method is apparent in these comparisons). They are however, accurate enough to draw qualitative conclusions about the effects of heat release on the growth of the two-dimensional mixing-layer, and other global features.

The final calibration of the code involves the overall validity of the chemistry models used in these studies. The full finite rate chemical kinetics model used previously by Drummond (ref. 10) was used as the standard for all comparisons. This model incorporates nine chemical species and eighteen reaction paths, with N_2 passive. The one-step chemistry model is nearly five times more efficient than the full chemistry model used for complete hydrogen-air combustion, and the abridged model is about twice as fast. The chemically reacting mixing-layer at a $M_c = 0.38$ between air and hydrogen seeded (10% mass) nitrogen was used to compare the models. The calculations were run to identical times on the same grid with the DCPS numerical method. Figures (4a-4e) show the spread of the layer based on the mean profiles as a function of spatial distance for five different quantities as calculated with each chemistry model: they are the 1) u velocity, 2) vorticity, 3) density, 4) H_2 mass fraction, and the 5) H_2O mass fraction. The global features of the velocity, vorticity and H_2O are both qualitatively and quantitatively similar. That the H_2O profiles compare so favorably is somewhat deceiving in these calculations. In comparing the ρ and H_2 mass fraction profiles, it is apparent that the one-step model is missing some of the more subtle features of the chemistry, and that the abridged reaction system is nearly identical to that of the full chemistry. Figure (4f) shows a comparison of the r.m.s. temperature profiles as calculated with each of the reaction models. Here it is apparent that the one-step model vastly overpredicts the temperature peaks in the system. The reasons for this are most likely a chemistry timescale which is too short and the inability of the one-step model to properly account for the endothermic molecular dissociation occurring in the reaction. Again, the abridged model is nearly identical with that of the full chemistry. It must be concluded from this study that the one-step model is only appropriate in representing global hydrodynamic features of the flow. The heat release and water production predicted by the model will only be qualitative. For calculations where the more subtle chemistry features of the flow are desired, then at least the abridged model must be used. In further calculations the one-step model was used when only heat release was important. For more detailed comparisons between non-reacting and reacting flows, the 7-7 model was used.

RESULTS AND DISCUSSION

The results presented here are for $M_c = 0.38$. The non-reacting case will be referred to as "n" and the reacting case as "r". Figure (5) shows the vorticity contour plot for both the cases "n" and "r". A direct comparison of the two cases shows that the early role-up of the layer occurring from x = 30mm to x = 50mm, is suppressed by the reaction. Further downstream, the length scale of the reacting case appears to be larger but the number and magnitude of vortical structures appear to be fewer than in the non-reacting case. Figure (6) shows the plots of the mean velocity and temperature, and their rms fluctuations. The growth of the layer is shown by the dotted lines. One can notice the distinct change of growth rate with distance. Recognizing that the first part of the growth is laminar, and the subsequent part transitional, similarity plots on the basis of the laminar and transitional similarity coordinates have been established (ref. 9).

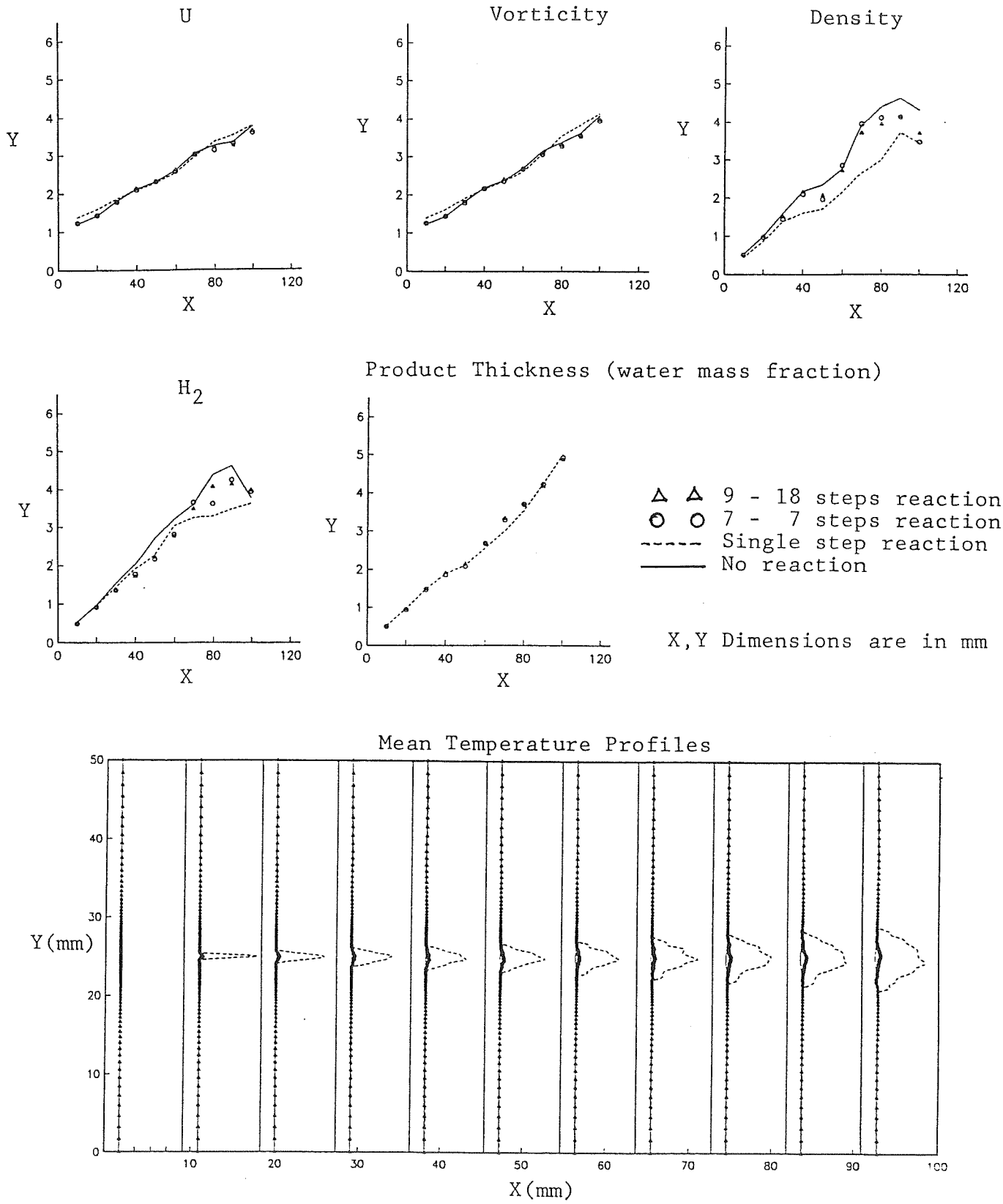

Figure 4: Comparison of the mean growth of (a) velocity, (b) vorticity, (c) density, (d) H_2, (e) H_2O and the (f) mean temperature profiles as calculated with the one-step, the abridged and full finite rate chemistry models.

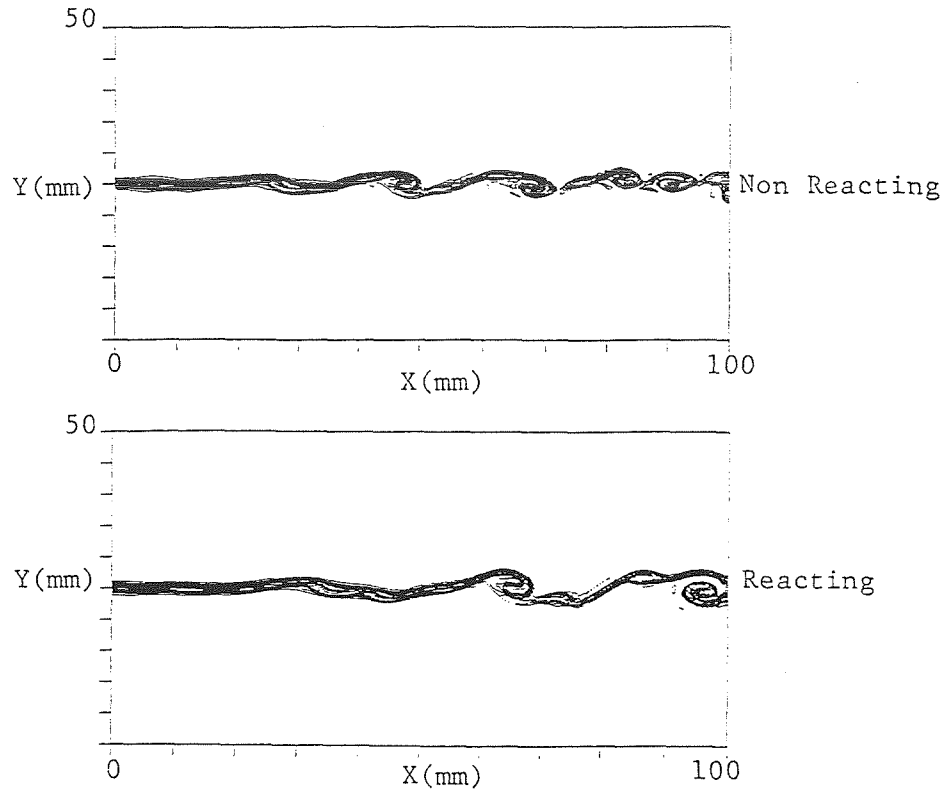

Figure 5: Comparison of vorticity contours for the a) "n" = no reaction, b) "r" = reaction.

The rms "u" fluctuations are shown in figure (6b) indicate that the maximum is about 6 %. There seems to be little difference in the location or magnitude of the fluctuations between the "n" and "r" cases. The development of the mean temperature profile shows that it peaks at about 2100 K and broadens with increasing x. The peak fluctuation goes to as high as 10 % of the mean for the case "r" and about 4 % for the case "n". The fluctuating values tend to grow with increasing distance in x, but are fairly uniform laterally across the layer. It is the large fluctuation with chemistry that produces a mean temperature which is low compared with the flame temperature. An examination of the temperature history at any x location shows that it is essentially at either the peak temperature of 2500 K (about half the theoretical increase predicted by an stiochiometric adiabatic flame temperature argument.) and the ambient of 2000 K with sharp transition. This picture is consistent with reaction being fast compared to flow times.

To help quantify this observation the concept of fractional residence time (α) is introduced. The mean temperature at any point is given in terms of the two temperatures, T_1 and T_0 by, $T_m = \alpha T_1 + (1-\alpha)T_0$. The root mean square fluctuation of temperature (T') is given by $T' = \sqrt{\alpha(T_1 - T_m)^2 + (1-\alpha)(T_m - T_0)^2}/\, T_m$. Examination of the data showed that the (α) at 2500 K remains at about 0.2 to 0.3 depending on the axial location. For the reacting case, T_1 = 2500 K, T_0 = 2000 K, α = 0.20, one gets T_m = 2100 K and T' = 0.10. These are the peak values of T_m and T' seen in the figure (6d), particularly in the downstream region. This model is consistent with the observation that mixing is centered around interfacial sheets within the vortical structures of the layer, and occupy a small fraction of the total mean width of the layer. By the same kind of arguments, for the nonreacting case for which T_1 = 1900 K, T_0 = 2000 K, α = 0.6, one obtains T_m = 1940 K and T' = 0.027. T_1 is taken as 1900 K because it is seen that in this case the local static temperature goes down to 1900 K due to gas dynamic expansion of the fluid locally. These results are also consistent with those seen in figure (6d) where the non-reacting flow shows the peak T' to be about 0.03.

A plot of the instantaneous p vs x at a specific y station for the M_c = 0.38 case is shown in figure (7a). Firstly, it can be noticed from this plot that the change in pressure is by no means insignificant. This results from both the initial perturbations and the large vortical forces in the layer. It changes from 0.07 to 0.14 MPa along x (as also along y through the shear layer). The plots of p vs x with reaction also show similar changes in pressure, without any other qualitative difference. The local Mach number plot with x shown in figure (7b) indicates that reaction reduces Mach number on an average. This is largely due to raise in acoustic speed due to increase in static temperature.

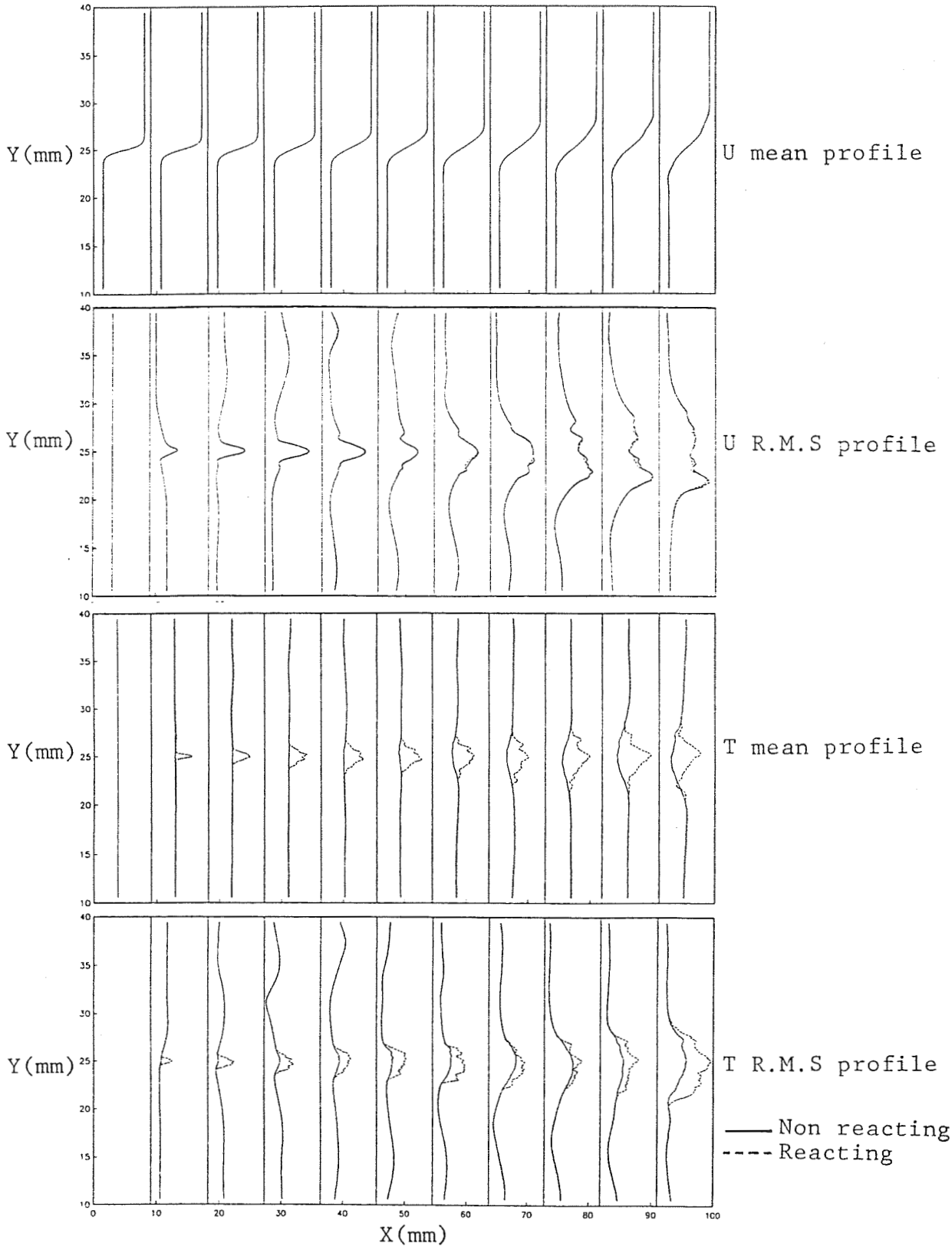

Figure 6: The plots of (a) u_m vs y , (b) rms u vs y, (c) T_m vs y, (d) rms T at various x stations.

The instantaneous pressure plots, at different times are used to obtain the convective speeds as discussed earlier. The results for the two cases at $M_c = 0.38$ are 1) "n", $u_c = 2260 \pm 50$ m/s and 2) "r", $u_c = 2083 \pm 50$ m/s. The theoretical speed calculated by equation (4) is 2150 m/s. The convective speed obtained here seems to be higher than that given by the formula by about 100 m/s at $M_c = 0.38$ The p-x curves have the same shape at different times, thus reflecting the truly constant speed of the structure. As reported by Mukunda et al. (ref. 9) and found in preliminary results here, for $M_c = 0.76$, the p-x curves change their shape even with in the characteristic sweep time. In addition, there is a variation in the speed of the structures computed at different times. It may well be that the concept of convective speed cannot be directly used to characterize the flow because the structures undergo dilatation to a large extent. Reaction seems to reduce the convective speed of the structures substantially - a 8.5 % (180 m/s) decrease at $M_c = 0.38$. This is expected to be a function of M_c. Again from preliminary calculations where the one-step chemistry model was used (with reservation) on $M_c = 0.76$, the heat release had a greatly reduced effect in lowering the convective speeds of the structures. This is not surprising since the increase in enthalpy is a much smaller percentage of the total enthalpy in the flow under the higher M_c conditions. At $M_c = 0.38$, the fractional increase in the instantaneous temperature is as much as 0.15 T_o and at $M_c = 0.76$, it is 0.25 T_o, whereas that due to combustion is 0.25 T_0. Thus as Mach number increases, changes due to gas dynamics become more relevant compared to those due to heat release.

Figure (7c) shows the variation of density (ρ) in the field. Firstly, it can be seen that the decrease in mean ρ is about 10 % due to heat release. This decrease in ρ is composed of that due to temperature, pressure and species mass fractions. In the experiments and analysis conducted elsewhere (ref. 2-5) on low Mach number flows with reaction, the free stream pressure of the two fluids is not significantly different while the local temperature rise is large compared with the ambient temperature. In these cases, the fractional change in ρ goes up to 0.4. In the present case, it is about 0.10 at the maximum.

Referring again to figures (4a-4e), plots of the thickness of the mixing-layer for the "n" and "r" cases are shown. In both cases, the growth of δ_u δ_ρ and δ_ω are around 4mm in 100mm. The mass fraction profiles grow from zero thickness and being passive scalars begin to acquire profiles similar to that of "u" at smaller x, and display an effective higher growth of 5mm in 100mm. The heat release seems to decrease the growth rate marginally. No appreciable difference between the "u" and vorticity growths are present. The Y_{H_2} growth shows a decrease of at least 10 %, but this is likely due to the consumption of H_2 by the reaction. The growth in the early stages is uniform but near the outflow plane, a drop in width occurs. These are due to coupling of the downstream region with initial disturbance pattern discussed earlier and also found in earlier work (ref. 5). From the ρ growth profiles it is seen that marginal reduction of the growth results from the chemical reaction (perhaps 10 %). It too shows spurious growth with axial distance due to the coupling effects of the inflow disturbance field. Figure (7d) shows the plot of Reynolds shear stress in the field. The Reynolds stresses with heat release are generally smaller than those without heat release. This contribution most likely comes from reduction in ρ. The decrease in the Reynolds stresses in the flow field due to heat release has been argued to be the cause of reduced growth of the shear-layer in incompressible flows. It seems unlikely that this could be the case in these calculations, due to the similarity between the "n" and "r" profiles.

In addition to the above, the time and space spectra of "u" fluctuations, kinetic energy of fluctuations, and vorticity fluctuations were examined for the "n" and "r" cases. The kinetic energy of fluctuations showed a 5 % decrease with the heat release, time and space spectra of "u" showed no discernible trends, and the vorticity distribution showed a marginal change.

It is appropriate now to discuss the present results in the light of earlier work. There are no experimental studies in supersonic reacting flows for comparison. However, there are many studies in incompressible flows referred to earlier. The principal conclusions of the work of Hermanson, Dimotakis (ref. 2,3) and McMurty et al. (ref. 5) are that the growth rate of the shear-layer decreases with the extent of heat release. A careful examination of the data indicates that the scatter in the data is not small though it may not invalidate the result that the layer thickness decreases with heat release. While most of their discussion centers around the growth variation with decrease in ρ due to heat release, some results of the growth rate variation with increase in the peak temperature is plotted. It is argued that the decrease in ρ causes dilatation and one would have to expect increase in growth rate. That the observed growth rate decreases - up to 10 % in the incompressible case and to a slightly lower extent in the present case at the same peak increment in temperature - is taken to indicate a decrease in entrainment of the fluid, to a larger extent (20-25 %).

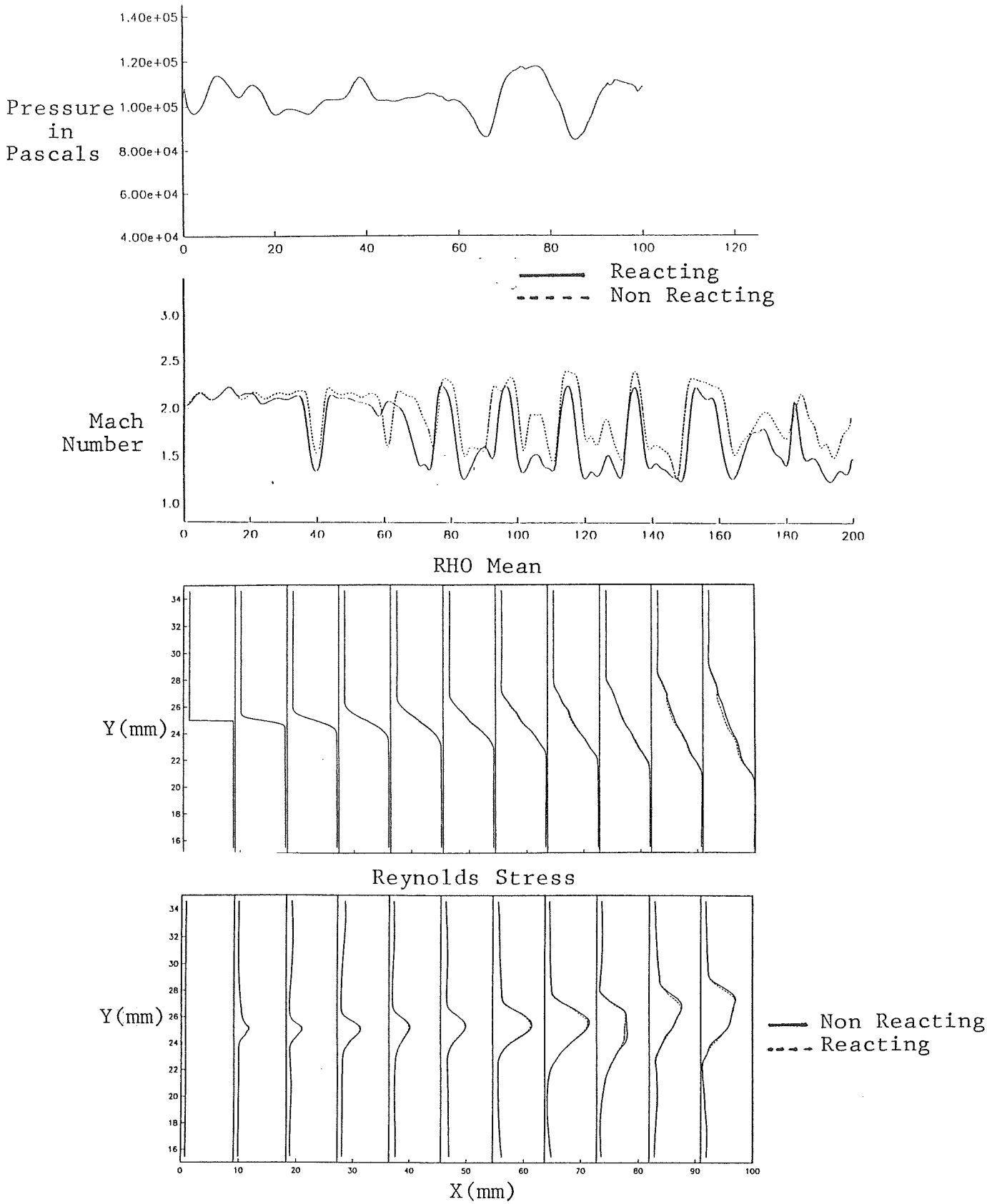

Figure 7: The variation of (a) static pressure with x ($y = y_m/2$), (b) Mach number with x ($y = y_m/2$), (c) ρ_m vs y at various x, (d) Reynolds stresses vs y at various x.

In the present case, the overall decrease in entrainment is estimated from the mass flux profiles to be 18 % at M_c = 0.38. The vortex core spacing in the case of non-reacting flow is about three times the layer thickness. This should be compared with values of about 1.5 in incompressible flows and 2-3 in high-speed flows (ref. 6). The enhanced core spacing in high-speed flows is argued to be due to a decreased rate of amplification of disturbances. This decreased rate causes the process of roll up to occur at a slower rate. Heat release causes a slight reduction in the vortex spacing (to about 2.5 δ) and causes the distinction between the vortical structures to be less clear (see figure (5)). Both these features have been discussed in incompressible flows (ref. 2).

CONCLUSIONS

In summary, high-speed reacting mixing-layers are characterized by a 'weak heat release' situation where gas dynamic interactions play a more substantial role in affecting the growth of the layer compared to incompressible flows. Specifically,

(1) The significant role of heat release is to reduce the growth rate of the mixing-layer by about 5-7 % and to reduce the convective speed of the structures by about 10 % at $M_c = 0.38$. Preliminary results indicate that increasing the convective Mach number will further reduce the effect of heat release.

(2) The density changes in the flow are caused by composition, pressure and temperature in the compressible case, unlike those in incompressible flows where temperature is the dominating factor. The reduction of entrainment in high-speed flows due to density changes is much less than in incompressible flows.

(3) Many phenomena like the reduction in Reynolds stresses, and kinetic energy of fluctuations due to heat release are akin to those in incompressible flows, but to a much lesser extent.

In view of the weaker role of heat release in affecting the dynamics of mixing-layers in high-speed flows, it is reasonable to conclude that it is useful to concentrate on non-reacting flows for the mixing related issues like enhanced mixing concepts. For many flows, heat release is likely to provide only a small perturbation to the non-reacting flow, and need not be a matter of major concern. Certainly, flow conditions exist where these conclusions may not be totally valid, and more work is needed in the area of three-dimensional chemically reacting flows. It is, however, believed that this work provides some useful guidelines on the behavior of high-speed chemically reacting mixing-layers.

REFERENCES

1. Brown, G.L. and Roshko, A., "On Density Effects and Large Structure in Turbulent Mixing Layers," *J.Fluid Mech.*, Vol. **91**, 319 - 335, (1974).

2. Hermanson, J.C. and Dimotakis, P.E., "Effects of Heat Release in a Turbulent, Reacting Shear Layer," *J.Fluid Mech.*, Vol. **199**, 333 - 375, (1989).

3. Dimotakis, P. E., "Turbulent Free Shear Layer Mixing," 27th Aerospace Sciences meeting, AIAA 89 - 0269, (1989).

4. McInville, R. M., Gatski. T. B., and Hassan. H, A., "Analysis of Large Vortical Structures in Shear Layers," *AIAAJ.*, Vol. **23**, 1165 -1171, (1985).

5. McMurtry, P.A., Riley, J.J. and Metcalfe, R.W. "Effects of Heat Release on the Large Scale Structures in a Turbulent Reacting Mixing Layer," *J.FluidMech*, Vol. **199**, 297 - 332, (1989).

6. Papamoschou, D and Roshko, A, "The Compressible turbulent Shear Layer," *J.FluidMech.*, Vol. **197**, 453-477 (1988); also see Papamoschou, D, "Structure of the Compressible Turbulent Shear Layer," AIAA Paper 89-0126, 27th Aerospace Sciences meeting, (1989).

7. Sandham, N and Reynolds, W., "The Compressible Mixing Layer: Linear Theory and Direct Simulation," 27th Aerospace Sciences meeting, AIAA 89-0371, (1989).

8. Lele, S,K., "Numerical Simulation of Compressible Free Shear Layer Flows," 27th Aerospace Sciences meeting, AIAA 89-0374, (1989).

9. Mukunda, H.S., Sekar, B., Carpenter, M., Drummond, J.P. and Kumar, A., Studies in the direct numerical simulation of high-speed mixing layers, NASA TP, to be released (1990).

10. Drummond, J.P. and Mukunda, H.S., Mixing enhancement in two-dimensional shear layers, NASA TM 1033, (1988).

11. Reynolds, W, C., "The Potential and Limitations of Direct and Large Eddy Simulations," Whither turbulence conference, Cornell Uni., March (1989).

12. Carpenter, M.H., "A Comparative Study of High Order, and Compact Numerical Algorithms with Existing Central and Upwind Algorithms," NASA TR in progress (1990).

13. Carpenter, M.H., "A Family of Compact Dissipative Two-Four Schemes," Submitted to the Journal of Computational Physics (1990).

14. Macaraeg, M.G., Streett, C.L., and Hussaini, M.Y., "A Spectral Collocation Solution to the Compressible Stability Eigenvalue Problem," NASA Technical Paper 2858, December (1988).

15. Gottlieb, and D. Turkel, E., "Dissipative Two-Four Methods for Time-Dependent Problems," *Mathematics of Computation*, Vol. **30**, No. 136, October, 703-723 (1976).